Ion beam doping of semiconductor nanowires

C. Borschel, R. Niepelt, S. Geburt, C. Ronning*
Institute for Solid State Physics, University of Jena
Carsten.Ronning@uni-jena.de

Abstract - **Semiconductor nanowires are of major importance within the area of nanotechnology, and are usually synthesized using the so-called vapor-liquid-solid mechanism. Controlled doping, a necessary issue in order to realize devices, is an unsolved problem and an extremely difficult task if using such a growth mechanism. We use an alternative route for modifying the electrical, optical and magnetic properties of semiconductor nanowires: ion implantation. Several independent studies on ion beam doping of semiconductor nanowires will be presented.**

I. INTRODUCTION

Semiconductor nanowires are frequently grown via the so-called vapor-liquid-solid (VLS) process, which has been already discovered for the growth of silicon whiskers using Au as catalyst in the 1960s and later on for compound semiconductors. However, the VLS growth model cannot be fully applied to the growth of compound semiconductor nanowires, because the more volatile component (usually the group V element in III-V semiconductors, or the group VI element in II-VI compounds) has almost no solubility within the catalyst used. Therefore, diffusion to the interface between catalyst and nanowires as well as a solid catalyst particle instead of a liquid one were introduced in order to explain the stoichiometric semiconductor whisker growth of some III-V compounds. Adding further components such as possible dopants to the growth process makes the prediction on the mechanism and the incorporation probability impossible. It is not clear, whether the dopants accumulate within the catalyst or they undergo diffusion mechanism from the sidewalls. As a result, reliable and well-controlled systematic doping studies are still lacking for semiconductor nanowires.

Doping using ion implantation has the advantages that both the incorporated dopant concentration as well as the dopant species can be controlled in an exact manner without the incorporation of any other elements, which is the main problem of doping upon growth of nanowires. Furthermore, all elements of the periodic table are available for ion beam doping experiments. The disadvantage of ion beam doping is the concurrent production of defects, which hamper the activation of the implanted impurities. However, in most common material systems like Si, GaAs, or ZnO the damage can be removed using post-implantation annealing procedures.

*Contacting Author: Carsten Ronning, University of Jena, Institute for Solid State Physics, Max-Wien-Platz 1, 07743 Jena, Germany

II. TM-DOPED ZNO NANOWIRES

Transition metal (TM) alloyed wide band gap semiconductors were predicted to show room temperature ferromagnetism with GaN and ZnO as the most promising candidates for spin-based electronic devices. Experimental data reveal inconsistent magnetic properties for TM alloyed ZnO, leaving the real mechanism for ferromagnetism in ZnO unclear. Nevertheless, the incorporation of TM centers results in a multiple splitting of degenerated 3d-shell states of free TM ions. The electronic structure is affected by the Stark effect of the crystal field, which has trigonal symmetry (C_{3V}) in hexagonal wurtzite structures like ZnO and is treated as perturbation of a tetrahedral (T_d) symmetry of a cubic crystal. Further splitting of the electronic structure results from spin-orbit interaction, vibrational contributions and Jahn-Teller coupling. As a result, transitions between these 3d-shell state become partly allowed and show very sharp transitions with long lifetimes (up to milliseconds). In addition to spintronic applications, these TM intra-shell transitions within semiconductors could be used in optoelectronic devices.

Zinc oxide nanowires were grown by vapour transport using the vapour liquid solid growth mechanism. The zinc oxide nanowires were implanted with transition metals (Co, Fe or Ni) and subsequently annealed [1,2]. Energy dispersive X-ray spectroscopy and electron energy loss spectroscopy measurements reveal a successful incorporation of the desired transition metals. Transmission electron microscopy analysis of implanted and annealed zinc oxide nanowires shows a strongly damaged zinc oxide lattice but no formation of transition metal-rich secondary phases. The as-grown nanowires show a strong and intensive near band edge emission and a moderately structured green luminescence band. After ion implantation, the structured green luminescence band increases in intensity and new sharp luminescence lines appear in the red luminescence region. Those sharp transitions are due to intra-shell 3d-transitions of iron and cobalt in the corresponding Fe- and Co-doped ZnO samples.

III. MN-DOPED ZNS NANOWIRES

ZnS nanostructures of different morphologies, i.e., nanowires and nanobelts, have been ion implanted with Mn and subsequently annealed to obtain $Zn_{1-x}Mn_xS$ nanostructures [3]. The Mn content x was adjusted to lie in the range from $4 \cdot 10^{-6}$% to 4% corresponding to a variation of the mean Mn-Mn distance between about 200 and 2 nm, respectively. The

$Zn_{1-x}Mn_xS$ nanowires have been studied by photoluminescence spectroscopy. The yellow Mn luminescence band indicates that the Mn^{2+} ions are incorporated on cation lattice sites replacing Zn. The temporal evolution of this internal $Mn^{2+}(3d^5)$ luminescence is measured over 4 orders of magnitude in intensity (see Fig. 1). The decay behaviour shows a clear dependence on the morphology of the nanostructure, in particular, on the ratio between the average Mn ion-killer centre distance and the characteristic lateral size of the nanostructure. If the mean Mn-Mn distance is comparable to or smaller than the average Mn ion-killer centre distance in the nanostructures, then concentration quenching of the Mn luminescence occurs similar to bulk. The non-exponential transients observed can be well described in the framework of a modified Förster model at reduced dimensionality. The photoluminescence (PL) behaviour of the nanowires loses its one-dimensional character when the mean Mn ion-killer centre distance becomes much smaller than the wire diameter. In contrast, the temporal PL behaviour of the nanobelts is only purely two dimensional in this case and is of intermediate character between one dimensional and two dimensional otherwise.

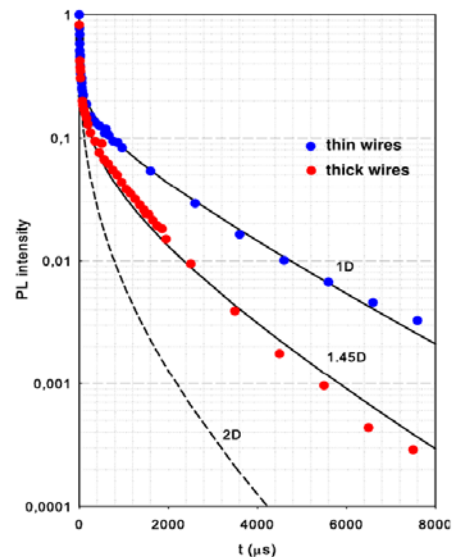

Fig. 1. Experimental decay curves of the Mn internal PL of thin wire- (blue) and thick belt-like (red) $Zn_{1-x}Mn_xS$ nanostructures with $x = 4 \cdot 10^{-6}$ % together with a fit (straight lines) using a modified Förster model. The effective morphology of the sample reflected by the PL decay behaviour is described by the fractional dimensionality D in the model. (Taken out of [3])

IV. Doping of Silicon Nanowires

The used Si nanowires have a relatively thick (5-10 nm) oxide shell surrounding a crystalline Si core ~10-20 nm in diameter [4]. After synthesis, the nanowires were mechanically transferred onto a 200 nm thick SiO_2 layer thermally grown on top of a heavily doped Si wafer, which can be used as back gate. Ion implantation was performed on these transferred wires. Source and drain contacts were then fabricated on individual NWs by e-beam lithography. The measured transfer curves of the field-effect transistors showed clear n- and p-type conduction type; thus, revealing successful doping with P and B at fluences as high as 10^{15} cm^{-2}. Contrary to what would happen in bulk Si for similar fluences, in SiNWs this only induces a limited amount of amorphization and structural disorder, as shown by both electrical transport and Raman measurements. We demonstrate that a fully crystalline structure can be recovered by thermal annealing at 800 °C. For not-annealed, as-implanted NWs, we correlate the onset of amorphization with an increase of phonon confinement in the NW core. This is ion-dependent and detectable for P-implantation only. Furthermore, a strong hysteresis for the transfer curves of the transistors was observed following both P and B implantation in the as-implanted situation.

In a second set of experiments [5], vertically aligned silicon nanowires were doped using ion implantation. Varying the fluences, acceleration voltages, and ions in subsequent implantation steps, uniform n- and p-type doping as well as p-n profiles are achieved along the nanowire axis. Electron beam-induced current (EBIC) imaging demonstrates the successful activation of the dopants, and current-voltage (I-V) characteristics show the rectifying behaviour of the p-n junctions.

V. Conclusions

We demonstrated that ion beam implantation is an appropriative tool for doping semiconductor nanowires, which is often difficult during growth. We showed that all properties (including electrical, optical as well as magnetical) of the nanowires can be specifically modified by the use of proper ion implantation and annealing conditions.

Acknowledgment

We thank all people listed below in our joint publications for their kind and outstanding collaborative work. This work is financially supported by the DFG under the contract Ro1198/7.

References

[1] C. Ronning, P.X. Gao, Y. Ding, and Z.L. Wang, "Manganese-doped ZnO nanobelts for spintronics", *Appl. Phys. Lett.*, vol. 84, pp. 783-785, 2004.

[2] S. Müller, M.J. Zhou, Quan Li, and C. Ronning, "Intra-shell luminescence of transition metal implanted zinc oxide nanowires", Nanotechnology, vol. 20, article no. 135704 , 2009.

[3] L. Chen, T. Niebling, W. Heimbrodt, D. Stichtenoth, C. Ronning, and P. J. Klar, "Dimensional dependence of the dynamics of the Mn 3*d*5 luminescence in (Zn, Mn)S nanowires and nanobelts", *Phys. Rev. B,* vol. 76, article no. 115325, 2007.

[4] A. Colli, A. Fasoli, C. Ronning, S. Pisana, S. Piscanec, and A. C. Ferrari, "Ion beam doping of silicon nanowires" *Nano Letters*, vol. 8, pp. 2188-2193, 2008.

[5] S. Hoffmann, J. Bauer, C. Ronning, Th. Stelzner, J. Michler, C. Ballif, V. Sivakov, and S. H. Christiansen, „Axial p-n Junctions Realized in Silicon Nanowires by Ion Implantation", *Nano Letters*, vol. 9, pp. 1341-1344, 2009.